Aminoguanidinium Hydrolysis Effected by a Hydroxo-Bridged Dicobalt(II) Complex as a Functional Model for Arginase and Catalyzed by Mononuclear Cobalt(II) Complexes

Chuan He and Stephen J. Lippard*

Contribution from the Department of Chemistry, Massachusetts Institute of Technology, Cambridge, Massachusetts 02139

Received July 25, 1997[⊗]

Abstract: The dinuclear complex $[Co_2(\mu\text{-OH})(\mu\text{-XDK})(bpy)_2(EtOH)](NO_3)$, where XDK is the dinucleating dicarboxylate ligand *m*-xylylenediamine bis(Kemp's triacid imide) and bpy = 2,2′-bipyridine, was prepared as a functional model for arginase. The substrate aminoguanidinium nitrate was hydrolyzed to urea in ethanol by the complex but not by free hydroxide ion under the same conditions. The amino group of the substrate binds to cobalt, as demonstrated by UV−vis spectroscopic studies. The syntheses of related dinuclear cobalt(II) complexes $[Co_2(\mu\text{-XDK})(NO_3)_2(CH_3OH)_2(H_2O)]$, $[Co_2(\mu\text{-Cl})(\mu\text{-XDK})(bpy)_2(EtOH)_2](NO_3)$, and $[Co_2(\mu\text{-XDK})(py)_3(NO_3)_2]$ are described. Mononuclear complexes $[Co(XDK)(bpy)(H_2O)]$ and $[Zn(XDK)(bpy)(H_2O)]$ were also prepared and characterized. The former catalytically hydrolyzes aminoguanidinium nitrate to urea in basic 1:1 methanol/water solutions, whereas the latter does not promote this reaction. Hydrolysis of aminoguanidinium ion is effected by $[Co(CH_3COO)_2]$ and $[Cu(CH_3COO)_2]$ in the presence of bpy, but not by $[Zn(CH_3COO)_2]$, $[Ni(CH_3COO)_2]$, or $[Mn(CH_3COO)_2]$ in the presence of bpy in 1:1 methanol/water solution. In all cases, coordination of the amino group of the substrate to the metal center under the reaction conditions may activate the leaving group and orient the guanidinium moiety close to the attacking nucleophile, metal-bound hydroxide ion, to promote the hydrolysis reaction.

Introduction

Metallohydrolases with carboxylate-bridged dinuclear metal centers have attracted considerable attention.[1−4] A variety of model compounds have been prepared to mimic the phosphatase and peptidase functions of the metalloenzyme.[5−12] Recently, the crystal structure of arginase, which catalyzes the hydrolysis of L-arginine to L-ornithine and urea, was reported.[13] This enzyme plays a key role in mammalian nitrogen metabolism and, together with NO synthase, regulates cytotoxic events dependent upon nitric oxide.[14,15] The active site of arginase contains two manganese(II) ions bridged by two carboxylate side chains of aspartate residues from the protein and a water molecule or hydroxide ion. From the three-dimensional structure of the arginase active site, a reasonable mechanism was proposed for arginine recognition and hydrolysis by metal-activated hydroxide ion.[13] Arginine is recognized and positioned by active site residues, Glu 277 in particular. A hydroxide group bridging two Mn(II) ions in the active site serves as the nucleophile which attacks the guanidinium moiety of the substrate, with protons being shuttled by nearby His and Asp residues. The enzyme is also activated by other divalent metal cations, especially Co(II).[16] A related enzyme which can cleave the guanidinium group is creatinase, or creatine amidinohydrolase, which converts creatine to sarcosine and urea.[17,18] Again the substrate creatine is firmly held in the active site of the enzyme by hydrogen bonding of its guanidinium and carboxylate groups to two Glu and two Arg protein side chains. These interactions position the guanidinium group toward a water molecule in the binding pocket, which performs the hydrolysis following deprotonation by a nearby His residue.

The structure of arginase has only appeared recently, and to our knowledge, no models of its guanidinium hydrolytic activity have been reported. Since hydrolysis of the guanidinium groups of arginine and creatine are key processes in the biological disposal of nitrogenous waste and the regulation of NO cytotoxicity, it is important to study and gain knowledge of this process.

[⊗] Abstract published in *Advance ACS Abstracts,* December 15, 1997.

(1) Lipscomb, W. N.; Sträter, N. *Chem. Rev.* **1996**, *96*, 2375−2433.
(2) Sträter, N.; Lipscomb, W. N.; Klabunde, T.; Krebs, B. *Angew. Chem., Int. Ed. Engl.* **1996**, *35*, 2024−2055.
(3) Wilcox, D. E. *Chem. Rev.* **1996**, *96*, 2435−2458.
(4) Dismukes, G. C. *Chem. Rev.* **1996**, *96*, 2909−2926.
(5) Jones, D. R.; Lindoy, L. F.; Sargeson, A. M. *J. Am. Chem. Soc.* **1983**, *105*, 7327−7336.
(6) Groves, J. T.; Baron, L. A. *J. Am. Chem. Soc.* **1989**, *111*, 5442−5448.
(7) Chin, J.; Zou, X. *J. Am. Chem. Soc.* **1988**, *110*, 223−225.
(8) Wahnon, D.; Lebuis, A. M.; Chin, J. *Angew. Chem., Int. Ed. Engl.* **1995**, *34*, 2412−2414.
(9) Koike, T.; Kimura, E. *J. Am. Chem. Soc.* **1991**, *113*, 8935−8941.
(10) Vance, D. H.; Czarnik, A. W. *J. Am. Chem. Soc.* **1993**, *115*, 12165−12166.
(11) Molenveld, P.; Kapsabelis, S.; Engbersen, J. F. J.; Reinhoudt, D. N. *J. Am. Chem. Soc.* **1997**, *119*, 2948−2949.
(12) Zhang, B.; Breslow, R. *J. Am. Chem. Soc.* **1997**, *119*, 1676−1681.
(13) Kanyo, Z. F.; Scholnick, L. R.; Ash, D. E.; Christianson, D. W. *Nature* **1996**, *383*, 554−557.
(14) Corraliza, I. M.; Soler, G.; Eichmann, K.; Modolell, M. *Biochem. Biophys. Res. Commun.* **1995**, *206*, 667−673.
(15) Daghigh, F.; Fukuto, J. M.; Ash, D. E. *Biochem. Biophys. Res. Commun.* **1994**, *202*, 174−180.
(16) Hellerman, L.; Perkins, M. E. *J. Biol. Chem.* **1935**, *12*, 175−194.
(17) Hoeffken, H. W.; Knof, S. H.; Bartlett, P. A.; Huber, R.; Moellering, H.; Schumacher, G. *J. Mol. Biol.* **1988**, *204*, 417−433.
(18) Coll, M.; Knof, S. H.; Ohga, Y.; Messerschmidt, A.; Huber, R.; Moellering, H.; Rüssmann, L.; Schumacher, G. *J. Mol. Biol.* **1990**, *214*, 597−610.

S0002-7863(97)02524-9 CCC: $15.00
Published on Web 01/14/1998

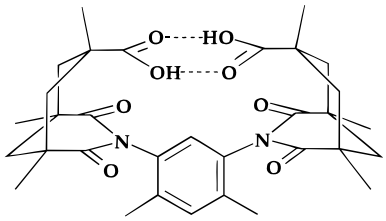

H_2XDK

Figure 1. Schematic representation of H_2XDK.

In the present work, we describe the synthesis and characterization of the hydroxo- and bis(carboxylato)-bridged dinuclear model compound $[Co_2(\mu\text{-OH})(\mu\text{-XDK})(bpy)_2(EtOH)](NO_3)$ (**2**), where H_2XDK = *m*-xylylenediamine bis(Kemp's triacid imide) (see Figure 1) and bpy = 2,2′-bipyridine.[19,20] The XDK ligand has been extensively employed in our laboratory to stabilize carboxylate-bridged dimetallic centers.[21−27] The syntheses of other dinuclear Co(II) complexes $[Co_2(\mu\text{-XDK})(NO_3)_2(CH_3OH)_2(H_2O)]$ (**1**), $[Co_2(\mu\text{-Cl})(\mu\text{-XDK})(bpy)_2(EtOH)_2](NO_3)$ (**3**), and $[Co_2(\mu\text{-XDK})(py)_3(NO_3)_2]$ (**4**) are also reported. Compound **2** effects the hydrolysis of aminoguanidinium ion to urea and hydrazine under conditions where free hydroxide ion is inactive. The substrate is catalytically hydrolyzed by $[Co(XDK)(bpy)(H_2O)]$ (**5**), $[Co(CH_3COO)_2]$, or $[Cu(CH_3COO)_2]$ with bpy but not by $[Zn(XDK)(bpy)(H_2O)]$ (**6**), $[Zn(CH_3COO)_2]$, $[Ni(CH_3COO)_2]$, or $[Mn(CH_3COO)_2]$ with bpy in basic 1:1 methanol/water solutions. The mechanisms of the hydrolysis reactions are discussed.

Experimental Section

General Procedures and Methods. All reagents were obtained from commercial suppliers and used without further purification unless otherwise noted. The reaction of aminoguanidinium nitrate with $[Mn(CH_3COO)_2]$ and bpy was carried out under an inert atmosphere by using standard Schlenk techniques. ^{1}H NMR spectra were taken on a Varian XL-300 spectrometer. Fourier-transform infrared spectra were recorded on a Bio-Rad FTS135 instrument. The compounds H_2XDK, Zn(XDK)·H_2O, and Na_2(XDK)·$4H_2O$ were prepared as previously described.[20,24,25]

$[Co_2(\mu\text{-XDK})(NO_3)_2(CH_3OH)_2(H_2O)]$ (1). A portion of $Co(NO_3)_2$·$6H_2O$ (130 mg, 0.447 mmol) was added to a solution of Na_2(XDK)·$4H_2O$ (150 mg, 0.215 mmol) in methanol (10 mL). The color of the solution changed from colorless to pink, and the reaction solution was stirred at room temperature for 1 h. The solvent was removed by a rotary evaporator, and the residue was redissolved in 1 mL of methanol. White inorganic salts were precipitated by addition of 5 mL of diethyl ether to this solution. The precipitates were filtered off, and the filtrate was concentrated to dryness by rotary evaporation. Recrystallization from diethyl ether/methanol (6:1) at −20 °C overnight yielded pink plates which were collected and washed with diethyl ether. The product rapidly turned into a purple powder upon drying in air. Drying under vacuum overnight yielded 130 mg (68% based on XDK) of the purple material **1**. X-ray quality pink crystals of $[Co_2(\mu\text{-XDK})(NO_3)_2(CH_3OH)_3(H_2O)_{1.625}]$·2.5MeOH·0.5$Et_2O$ were obtained by recrystallization from diethyl ether/methanol (6:1) at room temperature. FTIR (KBr cm^{-1}): 3480 (br), 3400 (br), 2922 (s), 2852 (s), 1716 (m), 1682 (s), 1643 (s), 1615 (m), 1377 (m), 1366 (m), 1284 (m), 1199 (m), 1021 (s), 959 (m), 851 (m), 765 (m). Anal. Calcd for $C_{34}H_{48}N_4O_{17}Co_2$: C, 45.24; H, 5.36; N, 6.21. Found: C, 44.85; H, 5.10; N, 6.34.

$[Co_2(\mu\text{-OH})(\mu\text{-XDK})(bpy)_2(EtOH)](NO_3)$ (2). A portion of 2,2′-bipyridine (33 mg, 0.210 mmol) was added to a solution of **1** (100 mg, 0.110 mmol) in methylene chloride (15 mL)/ethanol (10 mL). The solution, which changed color from pink to yellow-brown, was stirred at room temperature for 30 min. To this solution was added 46 μL of a methanolic solution of $(Me_4N)OH$ (25 wt %, d = 0.866 g mL^{-1}, 0.110 mmol) and the color turned brown-pink. After 1 h of stirring at room temperature, the solution was concentrated to dryness by rotary evaporation. The residue was extracted with 10 mL of methylene chloride, and the insoluble inorganic salts were filtered off. The filtrate was concentrated to dryness and redissolved in 1 mL of ethanol. Vapor diffusion of diethyl ether into this ethanol solution gave brown, block-shaped crystals of $[Co_2(\mu\text{-OH})(\mu\text{-XDK})(bpy)_2(EtOH)](NO_3)$·2EtOH suitable for X-ray crystallography, which were collected and washed with diethyl ether. Drying under vacuum overnight yielded 40 mg (34% based on **1**) of product. FTIR (KBr, cm^{-1}): 3520 (br), 2970 (m), 2929 (m), 1739 (m), 1685 (s), 1600 (s), 1360 (m), 1196 (s), 959 (m), 852 (m), 737 (m). UV−vis (EtOH) [λ_{max} (ϵ, M^{-1} cm^{-1})]: 470 nm (59), 502 nm (68), 800 nm (br, ∼3). Anal. Calcd for $C_{54}H_{61}N_7O_{13}Co_2$: C, 57.20; H, 5.42; N, 8.65. Found: C, 56.74; H, 5.01; N, 8.86.

$[Co_2(\mu\text{-Cl})(\mu\text{-XDK})(bpy)_2(EtOH)_2](NO_3)$ (3). To a solution of **1** (75 mg, 0.083 mmol) in methanol (5 mL)/methylene chloride (5 mL) were added 2,2′-bipyridine (28 mg, 0.181 mmol) and $(Et_4N)Cl$ (13.6 mg, 0.083 mmol). The reaction mixture was stirred for 30 min at room temperature, then the solution was concentrated to dryness by rotary evaporation. The residue was redissolved in 1 mL of ethanol, and vapor diffusion of diethyl ether into this solution yielded X-ray quality pink blocks of $[Co_2(\mu\text{-Cl})(\mu\text{-XDK})(bpy)_2(EtOH)_2](NO_3)$·3EtOH, which were collected, washed with diethyl ether, and air-dried (50 mg, 47% based on **1**). FTIR (Nujol, cm^{-1}): 3063 (br), 2962 (m), 2930 (m), 2879 (m), 1726 (m), 1692 (s), 1600 (s), 1560 (m), 1507 (m), 1358 (m), 1185 (m), 1022 (m), 982 (m), 957 (m), 887 (m), 851 (m), 762 (m), 736 (m). Anal. Calcd for **3**·EtOH·$2H_2O$, $C_{58}H_{76}N_7O_{16}ClCo_2$: C, 54.40; H, 5.98; N, 7.66. Found: C, 54.65; H, 5.86; N, 7.84.

$[Co_2(\mu\text{-XDK})(py)_3(NO_3)_2]$ (4). A portion of $Co(NO_3)_2$·$6H_2O$ (131 mg, 0.450 mmol) was added to a solution of Na_2(XDK)·$4H_2O$ (150 mg, 0.215 mmol) in methanol (15 mL). The color of the solution changed from colorless to purple, and the reaction solution was stirred at room temperature for 30 min. A portion of pyridine (1 mL) was added, and the solution was stirred for another 30 min. The solvent was removed by rotary evaporation, and the residue was extracted with methylene chloride (5 mL). The insoluble inorganic salts were filtered off, and the filtrate was concentrated to dryness. The residue was crystallized from MeOH (1 mL)/Et_2O (5 mL)/hexane (0.5 mL) at −20 °C to afford purple needles which were collected, washed with diethyl ether, and dried under vacuum overnight (200 mg, 88% based on XDK). Recrystallization of **5** from MeOH/Et_2O/hexane at room temperature gave block-shaped crystals of $[Co_2(\mu\text{-XDK})(py)_3(NO_3)_2]$·MeOH·0.5$Et_2O$ suitable for X-ray crystallography. FTIR (KBr, cm^{-1}): 3400 (br), 2971 (s), 2930 (m), 1739 (m), 1680 (s), 1603 (s), 1500 (s), 1363 (m), 1294 (m), 1195 (s), 1204 (m), 959 (m), 851 (m), 764 (m), 701 (m). Anal. Calcd for **4**·MeOH, $C_{48}H_{57}N_7O_{15}Co_2$: C, 52.90; H, 5.27; N, 9.00. Found: C, 52.71; H, 5.19; N, 8.96.

$[Co(XDK)(bpy)(H_2O)]$ (5). To a solution of Na_2XDK·$4H_2O$ (200 mg, 0.287 mmol) in methanol (10 mL)/methylene chloride (5 mL) were added $Co(NO_3)_2$·$6H_2O$ (100 mg, 0.344 mmol) and 2,2′-bipyridine (67 mg, 0.431 mmol). This reaction mixture was stirred at room temperature for 30 min. The solvent was removed by rotary evaporation, and the orange-pink residue was dissolved in methylene chloride (15 mL). The insoluble inorganic salts were filtered off, and the filtrate was washed with 4 × 20 mL portions of water. The organic layer was collected, dried with anhydrous sodium sulfite, and then concentrated to dryness and washed with diethyl ether. Drying under vacuum

(19) Kemp, D. S.; Petrakis, K. S. *J. Org. Chem.* **1981**, *46*, 5140−5143.
(20) Rebek, J., Jr.; Marshall, L.; Wolak, R.; Parris, K.; Killoran, M.; Askew, B.; Nemeth, D.; Islam, N. *J. Am. Chem. Soc.* **1985**, *107*, 7476−7481.
(21) Goldberg, D. P.; Watton, S. P.; Masschelein, A.; Wimmer, L.; Lippard, S. J. *J. Am. Chem. Soc.* **1993**, *115*, 5346−5347.
(22) Watton, S. P.; Masschelein, A.; Rebek, J., Jr.; Lippard, S. J. *J. Am. Chem. Soc.* **1994**, *116*, 5196−5205.
(23) Yun, J. W.; Tanase, T.; Pence, L. E.; Lippard, S. J. *J. Am. Chem. Soc.* **1995**, *117*, 4407−4408.
(24) Tanase, T.; Yun, J. W.; Lippard, S. J. *Inorg. Chem.* **1995**, *34*, 4220−4229.
(25) Tanase, T.; Lippard, S. J. *Inorg. Chem.* **1995**, *34*, 4682−4690.
(26) Tanase, T.; Yun, J. W.; Lippard, S. J. *Inorg. Chem.* **1996**, *35*, 3585−3594.
(27) Herold, S.; Lippard, S. J. *J. Am. Chem. Soc.* **1997**, *119*, 145−156.

Table 1. Summary of X-ray Crystallographic Data

	1·2.5MeOH·0.5Et_2O	**2**·2EtOH	**3**·3EtOH	**4**·MeOH·0.5Et_2O	**5**·3H_2O·0.5EtOH	**6**·1.25H_2O
formula	$C_{38.25}H_{65.75}N_4O_{20.38}Co_2$	$C_{58}H_{73}N_7O_{15}Co_2$	$C_{62}H_{84}N_7O_{16}ClCo_2$	$C_{50}H_{62}N_7O_{15.5}Co_2$	$C_{43}H_{57}N_4O_{12.5}Co$	$C_{42}H_{50.5}N_4O_{10.25}Zn$
fw	1025.56	1226.09	1336.67	1126.93	888.86	840.73
cryst system	triclinic	monoclinic	orthorhombic	monoclinic	monoclinic	monoclinic
space group	$P\bar{1}$	$P2_1/c$	*Pnma*	$P2_1/n$	$P2_1/c$	$P2_1/n$
a, Å	11.6456(2)	12.3880(4)	25.5097(5)	18.0846(4)	13.3115(4)	10.8213(4)
b, Å	18.8160(2)	16.7383(6)	17.9514(4)	12.3862(3)	15.7291(5)	22.4132(8)
c, Å	23.1313(5)	27.9451(10)	14.1510(3)	25.9939(5)	22.0887(7)	17.0439(6)
α, deg	70.3790(10)					
β, deg	89.5860(10)	94.1760(10)		102.7790(10)	91.4190(10)	101.9740(10)
γ, deg	85.6410(10)					
V, Å^3	4759.59(14)	5778.5(3)	6480.2(2)	5678.4(2)	4623.5(2)	4043.9(3)
Z	4	4	4	4	4	4
T, °C	−85	−85	−85	−85	−85	−85
ρ_{calcd}, g cm^{-3}	1.431	1.409	1.370	1.318	1.277	1.381
μ(Mo Kα), mm^{-1}	0.777	0.648	0.625	0.653	0.435	0.671
2θ range, deg	3−46	3−45	3−56	3−45	3−45	3−56
total no. of data	20697	22848	37716	23083	18268	24884
no. of unique data	12236	7109	7790	7252	5752	9403
no. of obsd data[a]	9044	4870	6075	6195	4195	7481
no. of params	1124	733	417	685	549	526
R^b	0.0597	0.0647	0.0518	0.0462	0.0661	0.0381
wR^2 [c]	0.1456	0.1328	0.1349	0.1382	0.1850	0.0991

[a] Observation criterion: $I > 2\sigma(I)$. [b] $R = \sum||F_o - F_c||/\sum|F_o|$. [c] $wR^2 = \{\sum[w(F_o^2 - F_c^2)^2]/\sum[w(F_o^2)^2]\}^{1/2}$.

overnight yielded 135 mg (58% based on XDK) of an orange-pink product. X-ray quality block-shaped crystals were grown from concentrated 1:1 methanol/H_2O solution. ^{1}H NMR (CD_2Cl_2): δ −25.90 (broad, assigned as 2 H from cobalt-bound water, since the signal disappeared after addition of D_2O), −3.02, −1.91, −1.62, 7.59, 8.17, 8.21, 14,11, 14.14, 28.00, 40.54, 47.50, 48.84, 49.63, 62.40. FTIR (KBr, cm^{-1}): 3408 (br), 3088 (m), 3076 (m), 2960 (s), 2926 (s), 2876 (m), 1745 (m), 1730 (m), 1681 (s), 1627 (m), 1445 (m), 1360 (m), 1200 (s), 959 (m), 852 (m), 761 (m). Anal. Calcd for $C_{42}H_{48}N_4O_9Co$: C, 62.14; H, 5.96; N, 6.90. Found: C, 61.77; H, 5.96; N, 6.77.

[Zn(XDK)(bpy)(H_2O)] (6). To a solution of Zn(XDK)·H_2O (200 mg, 0.302 mmol) in methanol (10 mL)/methylene chloride (10 mL) was added 2,2′-bipyridine (51 mg, 0.327 mmol). After the mixture was stirred at room temperature for 30 min, the solvent was removed by rotary evaporation and the white residue was dissolved in methylene chloride (10 mL). An insoluble white residue was filtered off, and the filtrate was washed with water (20 mL) three times. The organic layer was dried over anhydrous sodium sulfite, and the solution was concentrated by a rotary evaporator to 1 mL. Addition of 2 mL of diethyl ether to this concentrated solution gave a white precipitate, which was collected and washed with diethyl ether. Drying under vacuum overnight yielded 120 mg (50% based on XDK) of product. Colorless block-shaped crystals suitable for X-ray crystallography study were grown from concentrated methanol/water solution. ^{1}H NMR (CD_2Cl_2): δ 0.65 (s, 6 H), 1.03 (d, 4 H, J = 13 Hz), 1.25 (s, 12 H), 1.41 (d, 2 H, J = 13 Hz), 1,94 (s, 6 H), 2.07 (d, 2 H, J = 13 Hz), 2.32 (broad, assigned as 2 H from zinc-bound water, since the peak disappeared after the addition of D_2O), 2.69 (d, 4 H, J =13 Hz), 7.16 (s, 1 H), 7.58 (s, 1 H), 7.61 (t, 2 H, J = 6 Hz), 8.05 (t, 2 H, J = 8 Hz), 8.13 (d, 2 H, J = 8 Hz), 9.04 (d, 2 H, J = 4 Hz). FTIR (KBr, cm^{-1}): 3500 (br), 2961 (m), 2929 (m), 1734 (m), 1685 (s), 1579 (m), 1356 (m), 1196 (s), 958 (m), 852 (m), 763 (m). Anal. Calcd for $C_{42}H_{48}N_4O_9Zn$: C, 61.65; H, 5.91; N, 6.85. Found: C, 61.82; H, 5.55; N, 7.05.

X-ray Crystallography. General Procedures. X-ray crystallographic studies were carried out on a Siemens CCD diffractometer with graphite-monochromatized Mo Kα radiation (λ = 0.710 73 Å) controlled by a pentium-based PC running the SMART software package.[28] Single crystals were mounted at room temperature on the ends of quartz fibers in Paratone N oil, and data were collected at 193 K in a stream of cold N_2 maintained by a Siemens LT-2A nitrogen cryostat. Data collection and reduction protocols are described in detail elsewhere.[29] The structures were solved by direct methods and refined on F^2 by using the SHELXTL software package.[30] In general, all non-hydrogen atoms were refined anisotropically. Hydrogen atoms were assigned idealized locations and given an isotropic thermal parameter 1.2 times the thermal parameter of the carbon atom to which they were attached. Empirical absorption corrections were applied to all structures using SADABS, part of the SHELXTL program package.[30] In most cases, the atoms of a disordered solvent molecule were refined isotropically without including hydrogen atoms. Relevant crystallographic information is summarized in Table 1.

Structure of [Co_2(μ-XDK)(NO_3)$_2$(CH_3OH)$_3$(H_2O)$_{1.625}$]·2.5MeOH·0.5Et_2O. Two molecules crystallized in the asymmetric unit. In one molecule, the nitrate bound to one cobalt ion was disordered; the other was well behaved. The disorder was modeled as a bidentate nitrate coordinating to Co(1) through O(1A) and O(3A) at three-quarters occupancy with a methanol C(3A)−O(7A) coordinating trans to O(3A) also at three-quarters occupancy, as shown in Figure S2 of the Supporting Information. At one-quarter occupancy were a monodentate nitrate bound to Co(1) through O(3B), an oxygen atom O(7C) from a water molecule in the trans position, and the methanol C(3B)−O(7B) at a new site (Figure S2). These disordered atoms were all refined with isotropic thermal parameters. All other non-hydrogen atoms were refined anisotropically, except for the lattice solvent molecules. The oxygen atom of a lattice methanol molecule was disordered over two positions, O(1sA) and O(1sB), and refined at half-occupancy. The carbon atom of another lattice methanol molecule was also disordered over two positions, C(3sA) and C(3sB), refined at 0.6 and 0.4 occupancy, respectively. The atoms of the other methanol molecule and a diethyl ether molecule in the lattice were all refined at half-occupancy. The largest peak in the final Fourier map was 0.90 e$^-$/Å,^{3} located between two lattice methanol molecules.

Structure of [Co_2(μ-OH)(μ-XDK)(bpy)$_2$(EtOH)](NO_3)·2EtOH. The positions of all non-hydrogen atoms were refined anisotropically, except for the lattice solvent molecules, which were refined with isotropic temperature factors. The oxygen atom of one solvent ethanol molecule in the lattice was disordered over three positions, O(1sA), O(1sB), and O(1sC), each refined at one-third occupancy. One carbon atom of this ethanol was disordered over two positions, C(2sA) and C(2sB), and refined at half-occupancy for each position. The other solvent ethanol molecule in the lattice showed the same type of disorder, the oxygen atom of which was modeled over three positions, O(2sA),

(28) *SMART: Version 4.0*; Siemens Industrial Automation, Inc.: Madison, WI, 1994.

(29) Feig, A. L.; Bautista, M. T.; Lippard, S. J. *Inorg. Chem.* **1996**, *35*, 6892−6898.

(30) *SHELXTL: Structure Analysis Program. 5.0*; Siemens Industrial Automation, Inc.: Madison, WI, 1995.

O(2sB), and O(2sC), each refined at one-third occupancy; the carbon atom was modeled over two positions, C(4sA) and C(4sB), refined at 0.6 and 0.4 occupancies, respectively. The largest peak in the final Fourier map was 0.68 $e^-/Å^3$ located in the vicinity of the nitrate counterion in the lattice.

Structure of $[Co_2(\mu\text{-Cl})(\mu\text{-XDK})(bpy)_2(EtOH)_2](NO_3)\cdot 3EtOH$. The positions of all non-hydrogen atoms were refined anisotropically, except for a disordered lattice nitrate ion and solvent molecules, which were refined with isotropic temperature factors. A crystallographic mirror plane passing through Cl(1) and the xylyl ring of XDK relates the two halves of the cation. Those atoms which sit on the mirror plane were refined with half-occupancy. The nitrate ion in the lattice was disordered across the mirror plane and refined at half-occupancy, except for one oxygen atom which was disordered over two positions, O(5sA) and O(5sB), and thus refined at one-quarter occupancy. One ethanol molecule in the lattice was disordered over two sets of three atoms, C(1sA), C(2sA), and O(1sA) and C(1sB), C(1sB), and O(1sB), refined at half-occupancy. The other ethanol was disordered around a crystallographic C_2 axis. Its oxygen atom O(2s) was refined at half-occupancy, and the carbon C(3s) atom was shared by both positions and refined at full occupancy. The largest peak in the final Fourier map was 0.75 $e^-/Å^3$ located in the vicinity of O(1sB).

Structure of $[Co_2(\mu\text{-XDK})(py)_3(NO_3)_2]\cdot MeOH\cdot 0.5Et_2O$. The positions of all non-hydrogen atoms were refined anisotropically, except for the solvent molecules, which were refined with isotropic temperature factors. A half-occupied diethyl ether molecule in the lattice was badly disordered and modeled with defined bond lengths and fractional occupancy. The largest peak in the final Fourier map was 0.75 $e^-/Å^3$ situated near the disordered diethyl ether molecule.

Structure of $[Co(XDK)(bpy)(H_2O)]\cdot 3H_2O\cdot 0.5EtOH$. The positions of all non-hydrogen atoms were refined anisotropically, except for the solvent molecules in the lattice, which were refined with isotropic temperature factors. One carbon atom of a half-occupied ethanol in the lattice was disordered over two positions, C(2sA) and C(2sB), and refined at 0.25 occupancy. The largest peak in the final Fourier map was 0.87 $e^-/Å^3$ located close to the oxygen atom of the lattice ethanol molecule.

$[Zn(XDK)(bpy)(H_2O)]\cdot 1.25H_2O$ (6). The positions of all non-hydrogen atoms were refined anisotropically, except for a water molecule in the lattice, which was refined with isotropic thermal parameters at one-quarter occupancy. The two hydrogen atoms of the coordinated water molecule were located from difference Fourier maps and refined isotropically. The largest peak in the final difference map was 0.67 $e^-/Å^3$ located close to the methyl group of the xylyl ring of XDK.

Hydrolysis of Aminoguanidinium Ion by $[Co_2(\mu\text{-OH})(\mu\text{-XDK})(bpy)_2(EtOH)](NO_3)$. The hydrolysis of aminoguanidinium nitrate by **2** was initiated when 500 μL of a 0.05 M solution of the substrate in ethanol was added to 500 μL of a 0.005 M solution of the complex in ethanol in a 37 °C incubator. At 5, 10, 30, 45, 60, 90, and 120 min intervals after the start of the reaction, 100−200 μL aliquots were taken out and quenched in 2 mL of a 1:3:6 $H_2SO_4/H_3PO_4/H_2O$ acid solution. The product urea was monitored as described below to follow the kinetics of the reaction.

Hydrolysis of Aminoguanidinium Ion by $[Co(XDK)(bpy)(H_2O)]$. All experiments were performed in 1 mL of a 1:1 methanol/water mixed solvent system incubated at 37 °C. Standard buffer conditions used were 0.10 or 0.25 M CHES for pH 8.5−9.5 [CHES = 2-(cyclohexylamino)ethanesulfonic acid] or 0.10 M HEPES for pH 7.5−8.0 [HEPES = 4-(2-hydroxyethyl)-1-piperazineethanesulfonic acid]. Aliquots (15−200 μL) were quenched with 2 mL of a 1:3:6 $H_2SO_4/H_3PO_4/H_2O$ acid solution at various time intervals following initiation of the reaction. The product urea was detected (see below) to determine the reaction rate. Initial rate constants were obtained by measuring urea generated 5 min after the start of the reaction. A typical procedure for the kinetics experiment is as follows. The reaction was initiated by injecting 500 μL of a 0.1 M aqueous aminoguanidinium nitrate solution (0.5 M CHES, pH 9.5) into a 500 μL solution of 0.005 M **5** in methanol, the final concentrations of aminoguanidinium nitrate, **5**, and buffer being 0.05, 0.0025, and 0.25 M, respectively. After incubation at 37 °C for 5 min, 100 μL of solution was quenched with 2 mL of acid solution and the urea produced was quantitated.

Hydrolysis of Aminoguanidinium Ion by Other Mononuclear Divalent Metal Complexes. Stock solutions (0.005 M) of different metal(II) acetates and 1 equiv of bpy in methanol were prepared. Hydrolysis was initiated by injecting 500 μL of a 0.1 M aqueous aminoguanidinium nitrate solution (0.5 M CHES, pH 9.5) into 500 μL of these stock solutions. The same reaction conditions described above were followed to monitor urea formation.

Urea Assays. Urea was assayed with α-isonitrosopropiophenone (ISPF) by using a literature procedure.[31,32] A calibration curve was first obtained by adding 100 μL of standard aqueous urea solutions [(1−8) × 10^{-3} M] to 2 mL of a 1:3:6 $H_2SO_4/H_3PO_4/H_2O$ acid mixture (v/v). Next, 100 μL aliquots of a 9% ISPF solutions in ethanol were added and the resulting mixtures heated for 30 min at 100 °C in the dark. After the solutions were cooled for 30 min in the dark, the absorbance at 545 nm was measured. This procedure was employed to analyze the urea produced in the hydrolysis reactions. In control experiments, aminoguanidinium nitrate and the various metal complexes were assayed separately by this method and in no case was an absorption at 545 nm recorded. When semicarbazide was assayed, less than 5% of the A_{545} absorbance afforded by the same concentration of urea was observed. This small amount of absorbance is attributed to trace levels of urea generated in a reaction of semicarbazide with the acid mixture employed in the assay. These controls indicate urea to be the major product of the hydrolysis reactions. In one case, catalysis by **5**, the urea produced was additionally confirmed by ^{1}H NMR spectroscopy. Hydrolysis of aminoguanidinium nitrate in MeOH/H_2O was quenched by adjusting the pH to 5 after 100 min. Solvents were evaporated and the solid residues redissolved in DMSO-d_6. A ^{1}H NMR resonance at 5.4 ppm indicated the presence of urea, and the amount of product urea was quantitated to be approximately the same as revealed by the colorimetric assay described above.

Results and Discussion

Synthesis and Structural Characterization of $[Co_2(\mu\text{-OH})(\mu\text{-XDK})(bpy)_2(EtOH)](NO_3)$ (2). The reaction of $Co(NO_3)_2\cdot 6H_2O$ (2 equiv) with $Na_2(XDK)\cdot 4H_2O$[25] in methanol and subsequent workup afforded the purple complex $[Co_2(\mu\text{-XDK})(NO_3)_2(CH_3OH)_2(H_2O)]$ (**1**) (eq 1). The IR spectrum

$$Na_2(XDK)\cdot 4H_2O + Co(NO_3)_2\cdot 6H_2O \xrightarrow{MeOH} [Co_2(\mu\text{-XDK})(NO_3)_2(CH_3OH)_2(H_2O)] \quad (1)$$

indicated the presence of XDK (1615−1716 cm^{-1}), nitrate ions (1284−1377 cm^{-1}) and hydroxyl groups of water and methanol (3400−3480 cm^{-1}). From this material, compound **2**, $[Co_2(\mu\text{-OH})(\mu\text{-XDK})(bpy)_2(EtOH)](NO_3)$, was assembled by addition of bpy and $(Me_4N)OH$ (eq 2). The structure of **2** is illustrated

$$[Co_2(\mu\text{-XDK})(NO_3)_2(CH_3OH)_2(H_2O)] \xrightarrow[2.\ 1Me_4NOH]{1.\ 2bpy} {}^{CH_2Cl_2/EtOH} [Co_2(\mu\text{-OH})(\mu\text{-XDK})(bpy)_2(EtOH)](NO_3) \quad (2)$$

in Figure 2 and selected bond lengths and angles are provided in Table 2. The two cobalt atoms are 3.265(1) Å apart, bridged by the two carboxylate groups of XDK and a hydroxide group. Distorted trigonal bipyramidal coordination geometry at Co(2) is achieved by further binding of a bidentate bpy molecule. The other cobalt atom, Co(1), is six-coordinate, having additional bidentate bpy and ethanol ligands.

Other Carboxylate-Bridged Dicobalt(II) Complexes. When 1 equiv of $(Et_4N)Cl$ was substituted for $(Me_4N)OH$ in eq 2, the

(31) Corraliza, I. M.; Campo, M. L.; Soler, G.; Modolell, M. *J. Immunol. M.* **1994**, *174*, 231−235.
(32) Satoh, P. S.; Ito, Y. *Anal. Biochem.* **1968**, *23*, 219−229.

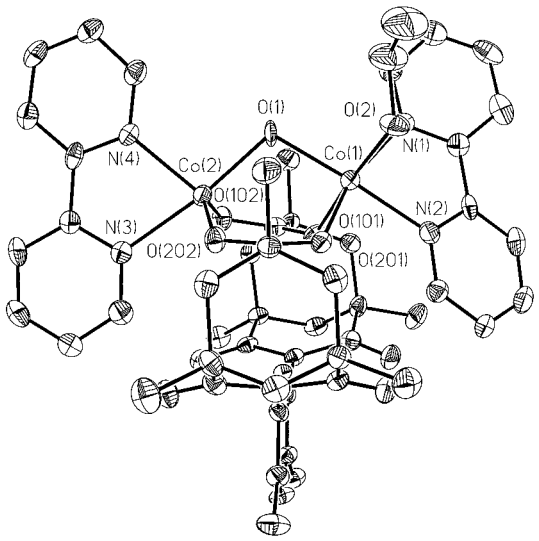

Figure 2. ORTEP diagram of $[Co_2(\mu\text{-OH})(\mu\text{-XDK})(bpy)_2(EtOH)](NO_3)$ (**2**) showing the 40% probability thermal ellipsoids for all nonhydrogen atoms.

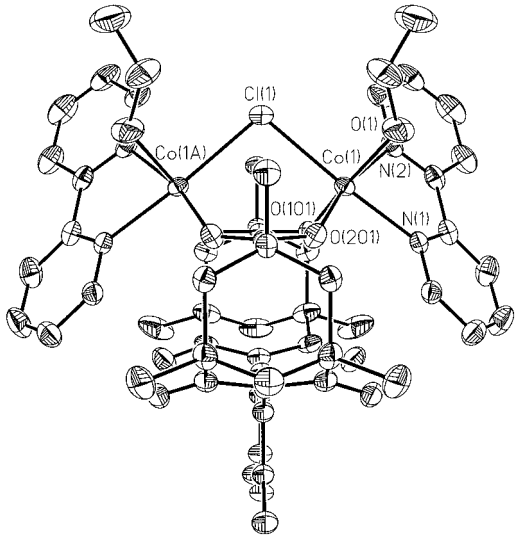

Figure 3. ORTEP diagram of $[Co_2(\mu\text{-Cl})(\mu\text{-XDK})(bpy)_2(EtOH)_2](NO_3)$ (**3**) showing the 40% probability thermal ellipsoids for all nonhydrogen atoms.

Table 2. Selected Bond Lengths (Å) and Angles (deg) for $[Co_2(\mu\text{-OH})(\mu\text{-XDK})(bpy)_2(EtOH)](NO_3)\cdot 2EtOH$ (**2**) and $[Co_2(\mu\text{-Cl})(\mu\text{-XDK})(bpy)_2(EtOH)_2]\cdot(NO_3)\cdot 3EtOH$ (**3**)[a]

bond lengths		bond angles	
		Compound **2**	
Co(1)···Co(2)	3.265(1)	Co(1)−O(1)−Co(2)	107.8(2)
Co(1)−O(1)	2.001(4)	O(1)−Co(1)−N(2)	172.8(2)
Co(1)−O(101)	2.125(4)	O(1)−Co(1)−N(1)	101.7(2)
Co(1)−O(201)	2.108(4)	O(1)−Co(1)−O(2)	94.0(2)
Co(1)−N(1)	2.198(5)	O(101)−Co(1)−O(201)	93.6(2)
Co(1)−N(2)	2.113(5)	O(201)−Co(1)−O(2)	84.9(2)
Co(1)−O(2)	2.173(4)	N(1)−Co(1)−N(2)	76.8(2)
Co(2)−O(1)	2.031(4)	O(1)−Co(2)−N(3)	173.0(2)
Co(2)−O(102)	2.030(4)	O(1)−Co(2)−N(4)	98.3(2)
Co(2)−O(202)	2.015(4)	O(102)−Co(2)−O(202)	132.5(2)
Co(2)−N(3)	2.198(5)	O(102)−Co(2)−N(4)	109.8(2)
Co(2)−N(4)	2.083(5)	O(202)−Co(2)−N(4)	113.2(2)
		N(3)−Co(2)−N(4)	74.7(2)
		Compound **3**	
Co(1)···Co(1A)	3.740(1)	Co(1)−Cl(1)−Co(1A)	98.68(3)
Co(1)−Cl(1)	2.465(1)	Cl(1)−Co(1)−N(1)	173.14(6)
Co(1)−O(101)	2.054(2)	Cl(1)−Co(1)−N(2)	97.02(7)
Co(1)−O(201)	2.052(2)	Cl(1)−Co(1)−O(1)	91.45(7)
Co(1)−N(1)	2.120(2)	O(101)−Co(1)−O(201)	101.24(7)
Co(1)−N(2)	2.158(2)	O(101)−Co(1)−O(1)	169.27(9)
Co(1)−O(1)	2.135(2)	N(1)−Co(1)−N(2)	76.28(8)

[a] Numbers in parentheses are estimated standard deviations of the last significant figure. Atoms are labeled as indicated in Figures 2 and 3.

chloride-bridged compound $[Co_2(\mu\text{-Cl})(\mu\text{-XDK})(bpy)_2(EtOH)_2](NO_3)$ (**3**) was obtained. An X-ray structure determination revealed C_s symmetry and octahedral coordination at each cobalt atom (Figure 3 and Table 2). The Co···Co distance of 3.740(1) Å is substantially greater than that in **2** because of the larger bridging chloride anion. The Co(1)−Cl(1)−Co(2) angle, 98.69(3)°, is about 10° less than the Co(1)−O(1)−Co(2) angle in **2**.

When a solution of **1** in methanol, generated by reaction of $Co(NO_3)_2\cdot 6H_2O$ with $Na_2(XDK)\cdot 4H_2O$, was treated excess pyridine, pink crystals of $[Co_2(\mu\text{-XDK})(py)_3(NO_3)_2]$ (**4**) were obtained. The structure was characterized by X-ray crystallography, an ORTEP drawing of which is given in Figure 4. Selected bond lengths and angles are listed in Table 3. Each cobalt atom is 6-coordinate and the Co···Co distance is 3.613(1) Å. The two cobalt atoms are bridged by two carboxylate groups

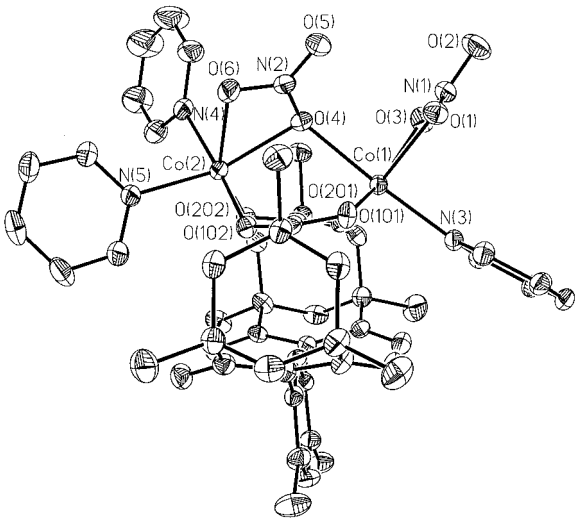

Figure 4. ORTEP diagram of $[Co_2(\mu\text{-XDK})(py)_3(NO_3)_2]$ (**4**) showing the 40% probability thermal ellipsoids for all nonhydrogen atoms.

from XDK and a nitrate ion. The bridging nitrate has an unusual coordination mode, with O(4) and O(6) chelating to Co(2) and O(4) linking two cobalt atoms. The distances are Co(1)−O(4), 2.238(3) Å; Co(2)−O(4), 2.161(3) Å; and Co(2)−O(6), 2.219(3) Å. This kind of coordination mode for nitrate, previously encountered in a few Cu(II), Ag(I), and Hg(II) complexes,[33−35] is more common in carboxylate-bridged dimetallic complexes.[36]

Hydrolysis of Aminoguanidinium Ion by $[Co_2(\mu\text{-OH})(\mu\text{-XDK})(bpy)_2(EtOH)](NO_3)$, Functional Model Chemistry for Arginase. In the proposed mechanism for arginine hydrolysis, the guanidinium group is positioned toward the bridging hydroxide ion by interactions with protein side chains in the vicinity of the active site (Scheme 1). Direct coordination of the guanidinium group to a metal ion is disfavored from

(33) Lindgren, T.; Sillanpää, R.; Rissanen, K.; Thompson, L. K.; O′Connor, C. J.; Van Albada, G. A.; Reedijk, J. *Inorg. Chim. Acta* **1990**, *171*, 95−102.
(34) Nardelli, M.; Pelizzi, C.; Pelizzi, G.; Tarasconi, P. *J. Chem. Soc., Dalton Trans.* **1985**, 321−331.
(35) Baker, L. J.; Bowmaker, G. A.; Healy, P. C.; Skelton, B. W.; White, A. H. *J. Chem. Soc., Dalton Trans.* **1992**, 989−997.
(36) Rardin, R. L.; Tolman, W. B.; Lippard, S. J. *New J. Chem.* **1991**, *15*, 417−430.

Table 3. Selected Bond Lengths (Å) and Angles (deg) for $[Co_2(\mu\text{-XDK})(py)_3(NO_3)_2]\cdot MeOH\cdot 0.5Et_2O$ (**4**) and $[Co(XDK)(bpy)(H_2O)]\cdot 3H_2O\cdot 0.5EtOH$ (**5**)[a]

bond lengths		bond angles	
		Compound **4**	
Co(1)···Co(2)	3.613(1)	Co(1)−O(4)−Co(2)	110.42(12)
Co(1)−O(101)	1.996(3)	O(1)−Co(1)−O(201)	150.78(12)
Co(1)−O(201)	1.991(3)	O(1)−Co(1)−O(4)	89.74(11)
Co(1)−O(1)	2.174(3)	O(1)−Co(1)−O(3)	58.95(11)
Co(1)−O(3)	2.204(3)	O(101)−Co(1)−O(201)	114.21(12)
Co(1)−N(3)	2.094(3)	O(101)−Co(1)−O(4)	87.83(11)
Co(1)−O(4)	2.238(3)	N(3)−Co(1)−O(4)	176.77(12)
Co(2)−O(102)	2.072(3)	O(4)−Co(2)−O(6)	59.15(11)
Co(2)−O(202)	2.046(3)	O(4)−Co(2)−N(4)	92.38(12)
Co(2)−O(4)	2.161(3)	O(4)−Co(2)−N(5)	156.53(13)
Co(2)−O(6)	2.216(3)	O(4)−Co(2)−O(102)	90.27(11)
Co(2)−N(4)	2.170(4)	O(6)−Co(2)−O(102)	87.71(11)
Co(2)−N(5)	2.111(3)	O(6)−Co(2)−O(202)	151.25(11)
		O(6)−Co(2)−N(4)	86.96(13)
		O(6)−Co(2)−N(5)	97.65(13)
		N(4)−Co(2)−N(5)	89.60(13)
		Compound **5**	
Co(1)−O(101)	1.989(4)	O(1)−Co(1)−N(1)	171.8(2)
Co(1)−O(201)	2.141(4)	O(1)−Co(1)−N(2)	94.7(2)
Co(1)−O(202)	2.179(4)	O(1)−Co(1)−O(101)	86.3(2)
Co(1)−O(1)	2.175(4)	O(1)−Co(1)−O(201)	88.0(2)
Co(1)−N(1)	2.111(5)	O(101)−Co(1)−O(201)	165.4(2)
Co(1)−N(2)	2.097(5)	O(101)−Co(1)−O(202)	106.5(2)
Co(1)···O(102)	3.440(4)	O(101)−Co(1)−N(1)	91.7(2)
O(1)···O(103)	2.819(6)	O(101)−Co(1)−N(2)	96.9(2)
O(1)···O(203)	2.875(6)	N(1)−Co(1)−N(2)	77.7(2)

[a] Numbers in parentheses are estimated standard deviations of the last significant figure. Atoms are labeled as indicated in Figures 4 and 7.

Scheme 1

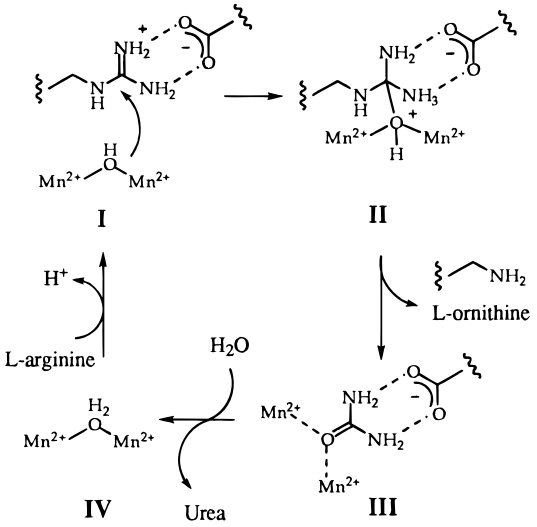

Coulombic considerations, although an interaction in the transition state cannot be excluded.[13] Instead of using carboxylate side chains in the second coordination sphere to position the guanidinium group, a strategy adopted in arginase and creatinase,[13,18] we decided to employ a substrate which can bind to the metal center and bring the guanidinium group close to the activated hydroxide ion. Aminoguanidinium nitrate was chosen for this purpose, since metal complexes of this ion have previously been synthesized.[37,38] The dinuclear complex **2** was used to model the active site of arginase because it has both the bridging nucleophile and a coordinated solvent molecule which could be displaced by substrate.

(37) Smith, G. S. *J. Chem. Soc.* **1937**, 1354−1358.
(38) Lieber, E.; Smith, G. B. L. *Chem. Rev.* **1939**, *25*, 216.

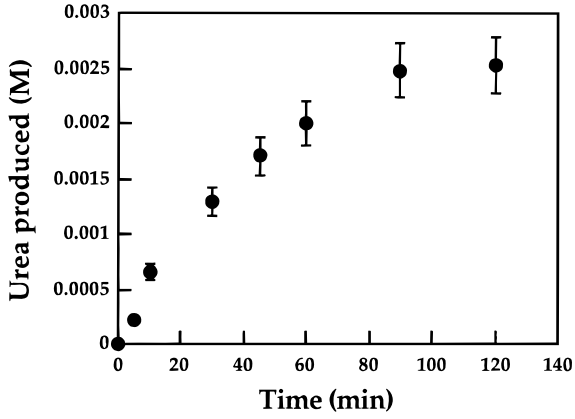

Figure 5. Hydrolysis of 0.025 M aminoguanidinium nitrate by 0.0025 M $[Co_2(\mu\text{-OH})(\mu\text{-XDK})(bpy)_2(EtOH)](NO_3)$ (**2**) at 37 °C in ethanol solution. The amount of urea generated was monitored for 2 h.

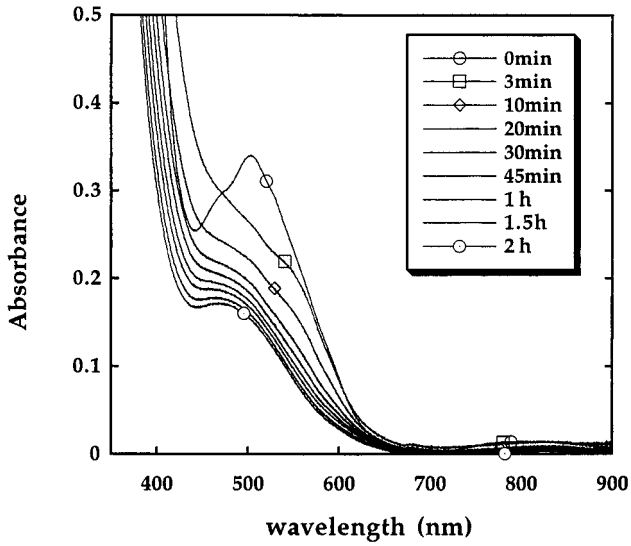

Figure 6. UV−vis studies of 0.025 M aminoguanidinium nitrate hydrolysis by 0.0025 M **2** in ethanol at 37 °C. Spectra were taken at 0, 3, 10, 20, 30, 45, 60, 90, and 120 min after 500 μL of 0.005 M aminoguanidinium nitrate ethanol solution was injected into 500 μL of 0.005 M **2** in ethanol to initiate the reaction.

Reaction of a 0.025 M solution of aminoguanidinium nitrate with 0.0025 M **2** in ethanol at 37 °C generated urea within 2 h, as shown in Figure 5. Since the bridging hydroxide ion was the only water-derived nucleophile available under the experimental conditions, the reaction was stoichiometric. The pseudo-first-order rate constant was determined to be $(4.4 \pm 0.4) \times 10^{-4}$ s^{-1} by fitting the experimental data to the appropriate expression. When 0.025 M aminoguanidinium nitrate was allowed to react in a control experiment with 0.0025 M tetramethylammonium hydroxide or 0.005 M sodium hydroxide under the same conditions, no detectable amount of urea was observed. After addition of aminoguanidinium nitrate to the ethanol solution of **2**, the UV−vis absorption spectrum changed immediately, indicating a change in cobalt(II) coordination. The UV−vis absorption spectral change, monitored for 2 h during hydrolysis, is shown in Figure 6.

Mechanisms considered for the hydrolysis reaction are depicted in Scheme 2. Aminoguanidinium ion first coordinates to the 6-coordinate cobalt(II) ion by displacing the coordinated solvent molecule. The hydroxide ion can either remain bridging (pathway a) or shift to a terminal position on the other cobalt ion (pathway b). Binding of the amino functionality to cobalt would orient the guanidinium moiety toward the hydroxide ion,

Scheme 2

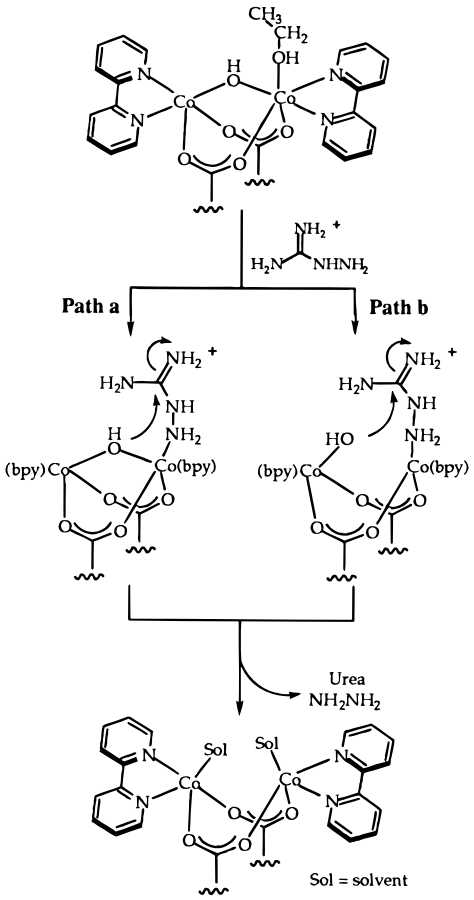

which might then attack the group intramolecularly, proceeding through a tetrahedral transition state and ultimately releasing urea and hydrazine. Cleavage of the C−N bond may also be facilitated by coordination of the amino group functionality to cobalt, rendering hydrazine a better leaving group.

Guanidinium nitrate could not be hydrolyzed by **2** in a control experiment, which is consistent with the notion that the guanidinium group was not positioned close enough to the nucleophile for hydrolysis to occur in the absence of the coordinating amino group. When aminoguanidinium nitrate was treated with free hydroxide ion in the absence of metal ions, the guanidinium group was similarly not reactive. Free hydroxide probably deprotonates the guanidinium group without performing nucleophilic attack on its carbon atom. Although the basicity of metal-bound hydroxide is substantially decreased compared to that of free hydroxide ion,[4] the fact that the aminoguanidinium ion can be hydrolyzed by **2** but not by OH^- indicates that metal-bound hydroxide is sufficiently nucleophilic to attack the guanidinium carbon atom of coordinated substrate.

Hydrolysis of Aminoguanidinium Ion Catalyzed by Mononuclear Divalent Metal Complexes. When **2**, which is insoluble in water, was dissolved in mixed alcohol (methanol, ethanol)/water solvent systems, one cobalt ion dissociated and [Co(XDK)(bpy)(H_2O)] (**5**) formed. This mononuclear complex was characterized by ^{1}H NMR, IR, and UV−vis spectroscopy as well as elemental analysis. Compound **5** can be prepared in a more direct manner by reacting $Na_2XDK\cdot 4H_2O$ with $Co(NO_3)_2\cdot 6H_2O$ and 2,2′-bipyridine. The crystal structure of material obtained by this route is shown in Figure 7, and selected bond lengths and angles are listed in Table 3. The cobalt ion in **5** has a distorted octahedral geometry, being coordinated by three oxygen atoms from XDK, two nitrogen atoms from bpy,

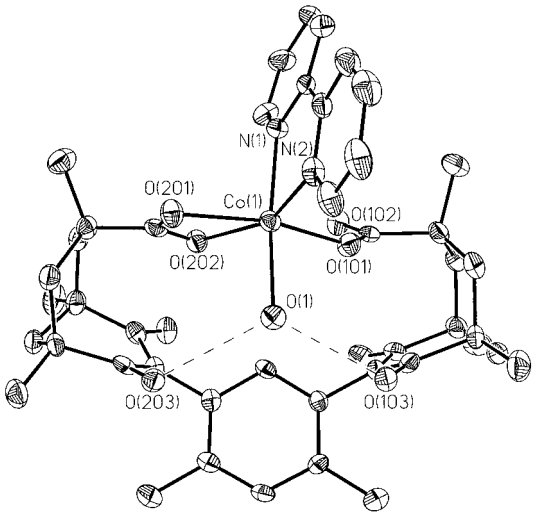

Figure 7. ORTEP diagram of [Co(XDK)(bpy)(H_2O)] (**5**) showing the 40% probability thermal ellipsoids for all nonhydrogen atoms.

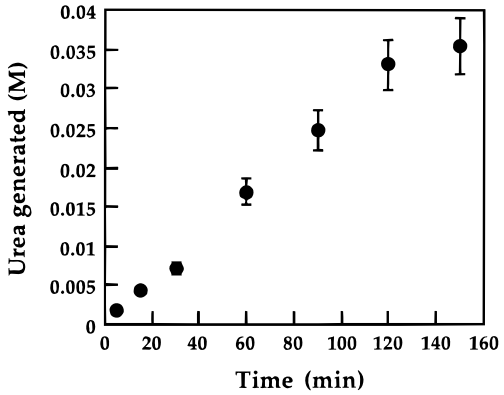

Figure 8. Hydrolysis of 0.05 M aminoguanidinium nitrate catalyzed by 0.0025 M [Co(XDK)(bpy)(H_2O)] (**5**) at 37 °C in a 1:1 MeOH/H_2O solution (0.25 M CHES buffer, pH 9.5). Product urea was detected for 14 turnovers.

and one oxygen atom from a bound water molecule. One carboxylate group of XDK is a bidentate chelate, with Co−O distances of 2.141(4) and 2.179(4) Å, whereas the other is monodentate with Co(1)−O(101) = 1.989(4) Å. Oxygen atom O(102) is out of bonding range, the Co(1)···O(102) distance being 3.440(4) Å. The two carboxylate groups are twisted by 27.6° with respect to one another. The cobalt-bound water molecule forms hydrogen bonds to two carbonyl oxygen atoms of the imides of the XDK ligand, O(1)···O(103) = 2.819(6) Å and O(1)···O(203) = 2.875(6) Å. The protons can be readily observed by ^{1}H NMR spectroscopy in CD_2Cl_2. The tridentate coordination of XDK in **5** resembles that reported previously for [Co(XDK)(neo)], where neo = neocuproine.[39] The latter compound, which contains a more sterically hindered ligand, was prepared in nonaqueous solvent and has distorted trigonal bipyramidal coordination geometry.

Compound **5** catalytically hydrolyzes aminoguanidinium ion in 1:1 methanol/water solution, as indicated in Figure 8. The amount of urea generated in this reaction was recorded for 14 turnovers, which took 2.5 h and proceeded with a pseudo-first-order rate constant of $(2.6 \pm 0.3) \times 10^{-3}$ s^{-1} at 37 °C. The hydrolysis rate increased at lower buffer concentrations, with 12 turnovers occurring in 1 h in 0.1 M CHES solutions at pH 9.5. This result indicates buffer inhibition of the catalytic

(39) Watton, S. P.; Davis, M. I.; Pence, L. E.; Rebek, J., Jr.; Lippard, S. J. *Inorg. Chim. Acta* **1995**, *235*, 195−204.

Scheme 3

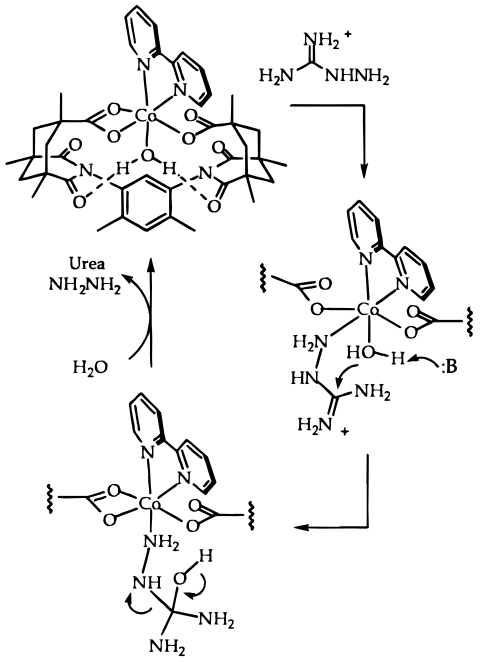

reaction. Control experiments were performed by reacting **5** with guanidinium nitrate under the same conditions, and no detectable urea was observed. No urea was produced from aminoguanidinium nitrate when **5** was not present in the reaction solution under the same conditions. UV−vis studies suggested a change in the Co(II) coordination sphere after addition of substrate to a solution of **5**, as for **2** above. Addition of guanidinium nitrate to a solution of **5** had no observable effect on the electronic absorption spectrum, which was monitored for 2 h under the same conditions.

A mechanism which accounts for these experimental results is proposed in Scheme 3. In the first step, aminoguanidinium ion coordinates to Co(II), replacing one of the cobalt-bound oxygen atoms of the bidentate XDK carboxylate group.[36,39] A water molecule, activated by coordination to cobalt and deprotonated by buffer or free hydroxide, performs a nucleophilic attack on the guanidinium group. Urea and hydrazine are produced, and the latter is displaced from cobalt by another water molecule to complete the catalytic circle. The switch from bidentate to monodentate ligation by one carboxylate group of XDK has been reported previously for mononuclear cobalt(II) and zinc(II) XDK complexes.[24,39]

The pH−rate profile of the reaction supports the suggestion that a metal-bound hydroxide ion is the active nucleophile (Figure 9). This species can attack the guanidinium carbon atom instead of deprotonating the guanidinium group because of the lower basicity, as discussed above for the stoichiometric reaction of **2**. Again, binding of the amino group to cobalt would position the guanidinium group toward the metal-bound nucleophile, a critical feature as revealed by the control experiments. Such coordination might also activate the leaving group because of the Lewis acidity of the metal ion. This combination of effects has been discussed previously, for example, to account for zinc-mediated phosphate ester hydrolysis.[40] The cobalt center delivers a coordinated hydroxide ion nucleophilically to the cobalt-bound aminoguanidinium ion and, at same time, helps stabilize the leaving group by interaction with its amino group. Although a mechanism involving hydrolysis of metal-bound

(40) Gellman, S. H.; Petter, R.; Breslow, R. *J. Am. Chem. Soc.* **1986**, *108*, 2388−2394.

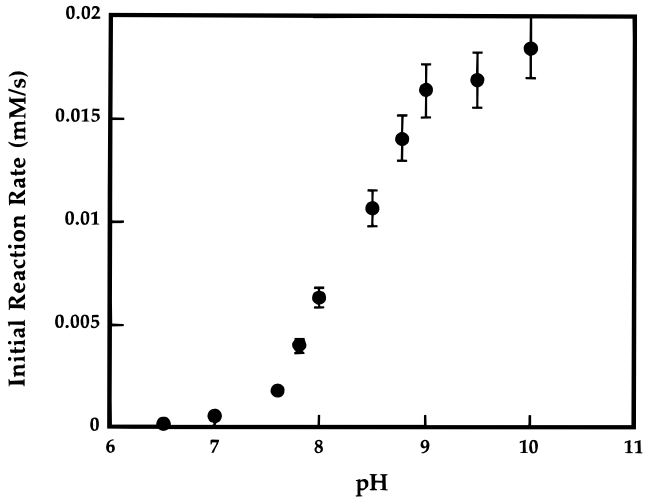

Figure 9. pH−rate profile for hydrolysis of 0.05 M aminoguanidinium nitrate by 0.0025 M **5** in a 1:1 MeOH/H_2O solution (0.1 M CHES for pH 8.5−9.5, 0.1 M HEPES for pH 7.5−8.0) at 37 °C. The initial reaction rate was obtained by determining the amount of urea produced after 5 min.

substrate purely by free hydroxide ion cannot be excluded, such a process is less likely considering the low concentration of this species.

The mononuclear complex [Zn(XDK)(bpy)(H_2O)] (**6**) was prepared by reacting 2,2′-bipyridine with ZnXDK·H_2O.[24] X-ray quality crystals were grown from saturated methanol/water solution, and an ORTEP drawing of the structure together with bond lengths and angles is supplied in the Supporting Information. The zinc ion has distorted trigonal bipyramidal geometry with two bipyridine nitrogen, two XDK carboxylate oxygen atoms, and a water molecule as donor ligands. The zinc-bound water is hydrogen bonded to the dangling carboxylate oxygen atoms of XDK, with O(1)···O(101) = 2.702(2) Å and O(1)···O(201) = 2.614(2) Å. No urea was detected when **6** was added to aminoguanidinium nitrate under the same reaction conditions used for **5**. The fact that there are no changes in the ^{1}H NMR resonances of **6** in these solutions indicates that the amino group of the aminoguanidinium ion may not be coordinating to zinc, which is consistent with the inability of **6** to promote its hydrolysis.

The effect of other simple metal acetate complexes in the presence of 1 equiv of bpy on the hydrolysis of the aminoguanidinium ion was also investigated. Hydrolysis could be promoted by cobalt(II) acetate or copper(II) acetate in the presence of 1 equiv of bpy under the same conditions. Solutions of the metal complexes changed color upon addition of aminoguanidinium nitrate, indicating coordination of the amino group to these metal ions. Zinc(II) acetate, nickel(II) acetate, or manganese(II) acetate did not promote the hydrolysis of aminoguanidinium group in basic methanol/water solutions in the presence of 1 equiv of bpy.[41] Table 4 summarizes these results.

The catalytic hydrolysis of aminoguanidinium ion by cobalt(II) or copper(II) acetate with 1 equiv of bpy is thought to go through the mechanism shown in Scheme 3. The zinc(II), nickel(II), or manganese(II) complexes may not bind aminoguanidinium ion under the conditions employed and thus not induce its hydrolysis. The failure of the manganese(II) complex to promote aminoguanidinium hydrolysis is inconsistent with

(41) Reaction of manganese(II) acetate with aminoguanidinium nitrate was performed in both pH 8.5 and pH 9.5 buffered 1:1 MeOH/H_2O solutions. A light yellow solid precipitated when the reaction was performed in pH 9.5 solution.

Table 4. Observed Initial First-Order Rate Constants for Aminoguanidinium Nitrate Hydrolysis

compound	$k_{obsd} \times 10^{-3}\,s^{-1}$, 0.10 M CHES	k_{obsd} x $10^{-3}\,s^{-1}$, 0.25 M CHES
5	5.8	2.7
6	no reaction[b]	no reaction[b]
$Co(CH_3COO)_2$ + bpy	8.2	3.8
$Cu(CH_3COO)_2$ + bpy	4.0	1.3
$Mn(CH_3COO)_2$ + bpy[c]	no reaction[b]	no reaction[b]
$Ni(CH_3COO)_2$ + bpy	no reaction[b]	no reaction[b]
$Zn(CH_3COO)_2$ + bpy	no reaction[b]	no reaction[b]

[a] In pH 9.5 1:1 MeOH/H_2O, 0.05 M aminoguanidinium nitrate reacting with 0.0025 M metal complexes at 37 °C incubation. [b] Reaction was monitored for 2 h. [c] In both pH 9.5 and pH 8.5 1:1 MeOH/H_2O.

its function in arginase. The role of the carboxylate-bridged dimanganese(II) center in arginase is to generate the active nucleophile. It does not bind directly to substrate,[4,13] an apparent requirement for the hydrolysis reactions investigated here, and one which manganese(II) failed to meet. The dimanganese(II) analogue of **2** has not yet been evaluated.

Summary and Conclusions

The guanidinium group of arginine and creatine stabilizes protein structure and assists in protein function. Its hydrolysis is a key step in several biochemical pathways. To model the role of the carboxylate-bridged dimetallic center in arginase and to study the metal-promoted hydrolysis of the guanidinium group, the hydroxobis(carboxylato)-bridged dinuclear complex $[Co_2(\mu\text{-OH})(\mu\text{-XDK})(bpy)_2(EtOH)](NO_3)$ (**2**) was prepared. The aminoguanidinium ion was stoichiometrically hydrolyzed by **2** in ethanol but not by free hydroxide ion under the same conditions. Mononuclear Co(II) and Cu(II) 2,2′-bipyridine/carboxylate complexes catalytically promoted the hydrolysis of aminoguanidinium ion under basic conditions in aqueous solution. Nature employs a dimanganese(II) site in arginase to hydrolyze the guanidinium moiety of arginine. The function of this dinuclear site is to generate an active nucleophile, since the pK_a of water is substantially lowered when it bridges two metal ions.[4] The guanidinium group of arginine is positioned toward the metal-bound nucleophile by interactions with protein side chain residues. In the present study, the amino group of aminoguanidinium binds to the metal centers, bringing the guanidinium group close to the metal-bound hydroxide ion to induce hydrolysis. The role of the metal ions here seems to deliver a metal-bound hydroxide nucleophile to the well positioned, metal-bound aminoguanidinium ion and possibly also to stabilize the leaving group by coordination to its amino functionality.

Acknowledgment. This work was supported by a grant from the National Science Foundation. We are grateful to Dr. P. Fuhrmann for help with the X-ray crystallography.

Supporting Information Available: Tables S1−S30, listing full crystallographic details, atomic coordinates, equivalent isotropic thermal and anisotropic temperature parameters, and bond distances and angles for **1**−**6**; Figure S1, displaying the numbering scheme for the XDK ligand; Figures S2 and S3, showing full ORTEP plots of two molecules of **1**; Figures S4−S8, displaying full ORTEP plots of **2**−**6**; Figures S9 and S10, presenting the hydrolysis of 0.05 M aminoguanidinium nitrate catalyzed by 0.0025 M **5** in 0.10 M, pH 9.5, CHES solution and UV−vis studies of this reaction; and Figure S11, showing the standard calibration curve for urea determination (80 pages). An X-ray crystallographic file, in CIF format, is available through the Internet only. See any current masthead page for ordering and Internet access instructions.

JA972524D